S 62. *The Oxides of Uranium.*

By K. B. Alberman and J. S. Anderson.

Phase equilibria in the uranium–oxygen system between the composition limits UO_2 and $UO_{2\cdot3}$ have been investigated in detail with regard both to the structure of the phases formed and to the kinetics of their formation from UO_2 and oxygen.

The dioxide, which possesses a fluorite structure, will take up oxygen at temperatures below 230° to a composition $UO_{2\cdot2}$ without change of structure or appreciable change of cell dimension. Oxides in this composition range disproportionate, when annealed at high temperature, into two well-defined cubic phases, *viz.*, UO_2 and a phase of composition close to $UO_{2\cdot2}$ (" β-UO_2 phase ").

Oxides in the composition range $UO_{2\cdot2}$—$UO_{2\cdot3}$ prepared below 230° have a tetragonal structure with axial ratio c/a changing progressively with composition; these oxides disproportionate on heating into the β-cubic phase and a U_3O_8-like phase.

Kinetic studies of the oxidation process suggest that oxidation proceeds by way of a diffusion-controlled reaction in a solid phase of variable composition.

These studies suggest a general similarity between the oxides of uranium and those of molybdenum and tungsten.

Uranium, like its congeners in Group VI of the Periodic Table, forms a large number of oxides, the relations between which have not yet been fully established. Biltz and Müller (*Z. anorg. Chem.*, 1927, **163**, 257), whose systematic study of the whole system summarises the position at that date, found that between the highest oxides UO_3 and U_3O_8 there was a considerable measure of mutual solid solubility; their conclusion that the U_3O_8 phase exists over a range of composition on both sides of the ideal formula appears to be substantiated by more recent work.

Between U_3O_8 and the well-defined dioxide, there is evidence for the existence of one or more intermediate oxides, but there has been little agreement on the compounds actually formed. Diuranium pentoxide, U_2O_5, has been reported by Péligot (*Ann. Chim. Phys.*, 1842, **5**, 23), Oechsner de Coninck (*Bull. Soc. chim.*, 1903, **28**, 6), and Schwartz (*Helv. Chim. Acta*, 1920, **3**, 344), but its existence has not, until recently at least, been established (cf. Ebelmen, *Ann. Chim. Phys.*, 1842, **5**, 200; Rammelsberg, *Pogg. Ann.*, 1843, **59**, 6; Remeté, *ibid.*, 1865, **124**, 126; Zimmermann, Alibegoff, and Kruss, *Annalen*, 1886, **232**, 283). It does not appear as an intermediate step in the tensimetric degradation of U_3O_8 (Biltz and Müller, *loc. cit.*) or in the reduction of U_3O_8 (Lebeau, *Compt. rend.*, 1922, **174**, 388; Jolibois and Bossuet, *ibid.*, p. 386). More recently, Lydén (*Finska Kemist. Medd.*, 1939, **48**, 124) has reported its formation by the selective leaching of UO_2^{2+} ions from U_3O_8. Rundle, Baenziger, Wilson, and MacDonald (*J. Amer. Chem. Soc.*, 1948, **70**, 99) have, apparently conclusively, characterised as U_2O_5 the product of reaction of equimolar quantites of UO_2 and U_3O_8. The oxides UO_3, U_3O_8, and U_2O_5 have a close structural relationship, being apparently based on a common framework of uranium atoms in the crystal lattice. We have found, in agreement with Rundle and his co-workers, that the reaction of UO_2 with U_3O_8 at 1000° forms a U_3O_8-like oxide, and it is clear that, contrary to the view expressed by Grønvold and Haraldsen (*Nature*, 1948, **162**, 69), U_2O_5 is quite distinct from the tetragonal UO_2-like phase discussed at length below.

Uncertainty also exists as to the possible range of composition of the UO_2 phase, and of the oxides related to it. Biltz and Müller (*loc. cit.*) found that in the reduction of U_3O_8 there was a discontinuity at a composition about $UO_{2\cdot25}$, and also that material having a similar composition was perceptibly volatile; they were, however, unable to detect any differences between the *X*-ray diffraction pattern of this material and that of pure UO_2. The latter is very readily oxidised at comparatively low temperatures, depending on its particle size. Finely divided material may, indeed, oxidise at the ordinary temperature (Hofmann and Höschele, *Ber.*, 1915, **48**, 21). Jolibois (*Compt. rend.*, 1947, **224**, 1393) observed that the oxidation of UO_2 at 220° came to a halt at the composition $UO_{2\cdot33}$ (U_3O_7) and proceeded further, to U_3O_8, only above 300°. The intermediate oxide, U_3O_7, he found to give an *X*-ray diffraction pattern like that of UO_2, but with additional lines. More recently, Grønvold and Haraldsen (*loc. cit.*) have stated that material prepared by Jolibois's method has a tetragonal structure, related to that of UO_2—a conclusion which we had already reached when Grønvold and Haraldsen's note appeared—but with the composition $UO_{2\cdot40}$, the UO_2 phase itself extending over a range of composition up to $UO_{2\cdot33}$. Rundle and his co-workers, however, assign to the UO_2 phase a limit of composition about $UO_{2\cdot25}$, well characterised by its cell dimensions. In neither case is evidence advanced as to the constitution of oxides intermediate between stoicheiometric UO_2 and the upper limit of composition.

This paper is based upon a detailed study of the course of oxidation of UO_2, and of the thermal stability of the products obtained thereby. It shows that the observations of Biltz and Müller, Rundle *et al.*, Jolibois, and Grønvold and Haraldsen are each broadly correct, though the composition limits assigned to the several phases, notably by Grønvold and Haraldsen, have not in every cases been confirmed. A tentative phase diagram can be advanced, showing the existence of two phases of variable composition which are either the stable phase at low temperatures ($<250°$) or, probably, altogether metastable with respect to UO_2 itself (here designated the α-UO_2 phase), and a second cubic oxide, related to UO_2, here termed the β-UO_2 phase, which exist at high temperatures. The sections of the work described in this paper cover an extensive *X*-ray study of the UO_2 system, together with some preliminary results on the kinetics of the oxidation of this oxide. A fuller discussion of the reaction kinetics in the system will be given later.

EXPERIMENTAL.

Preparation of Oxides.—The starting material for the various oxides prepared during this work was a very pure grade of UO_2. This oxide had a nominal particle size of 5 μ. An examination with the electron microscope, kindly carried out for us by Dr. C. S. Lees, of the General Physics Division, A.E.R.E., revealed, however, that the 5 μ.-particles were themselves secondary aggregates of much smaller particles. The primary particles appeared to be well-formed crystallites, 0·1—0·2 μ. or less in size, their outline suggested (100) and (111) as the most frequently developed faces, and interpenetrating cubes were common. The ultramicroscopic crystals of UO_2 closely resemble the macroscopic habit of fluorite, as figured in Miers's " Mineralogy." Oxides of known composition were prepared from this material by oxidising it in air or oxygen in a thermostatically controlled oven at temperatures between 120° and 250°. The UO_2 was spread in a thin layer in silica or aluminium dishes and the composition was calculated from measurement of the increase in weight. The compositions given are probably accurate to $\pm 0{\cdot}001$ atom of oxygen per formula weight. Some of the specimens were obtained in the course of kinetic measurements and their oxygen content was determined from gas volumetric data.

Treatment of Oxides.—*X*-Ray diffraction studies were made of the oxides: (*a*) As prepared, without subjecting them to any process of homogenisation—these materials give, nevertheless, every evidence of being single-phase materials. (*b*) After subjection to annealing processes at high temperatures.

For prolonged annealing, the oxides were sealed in evacuated silica tubes. Shorter annealings were carried out in dynamic vacuum, at temperatures from 500° to 1000°. Heatings above 1000° were carried out in zirconia crucibles in a small tungsten-spiral vacuum furnace. In annealing processes carried out in a sealed tube, any oxygen evolved by the material was retained in the system, so that the net composition was not altered. In the vacuum-furnace annealings, especially at the high temperatures, phases with an appreciable dissociation pressure of oxygen were ultimately degraded to UO_2.

X-*Ray Measurements.*—Samples were exposed in thin-walled Pyrex capillaries of about 0·3-mm. bore, most of the work being done on a 9-cm. Unicam camera. The annealed oxides gave good resolution of the copper K_{α_1}–K_{α_2} doublet. With the unannealed oxides, the patterns were rather diffuse, but the high-angle reflections were usually suitable for measurement. The lattice parameter of the cubic phases was in every case extrapolated by Jay and Bradley's method (*Proc. Physical Soc.*, 1932, **44**, 563). The precision of the final values is probably $\pm 0{\cdot}002$ X.U. The tetragonal phases were photographed on a 19-cm. Unicam camera. Since the departure from cubic symmetry is only very small, the photographs could conveniently be indexed by reference to the basic UO_2 diffraction pattern, the measurements being ultimately combined by a " least squares " method to find the axial ratio. These materials were necessarily prepared in every case at low temperatures, and gave patterns with diffraction lines rather too broad for optimum measurement. The axial ratios and cell dimensions of the tetragonal phase are accordingly rather sensitive to experimental errors.

DISCUSSION.

The following table summarises the relation between composition, thermal history, constitution, and cell dimensions for preparations ranging in composition between UO_2 and $UO_{2{\cdot}3}$. It is convenient to discuss the constitution of the annealed and the unannealed preparations separately; since the unannealed oxides show a change from cubic to tetragonal symmetry at some composition around $UO_{2{\cdot}2}$, the discussion of the low-temperature oxides has been further subdivided.

(I) *Low-temperature Oxides in the Composition Range* $UO_{2{\cdot}0}$ *to* $UO_{2{\cdot}20}$.—Oxides having compositions in this range are cubic; their diffraction patterns show no displacement, systematic broadening, or changes in the relative intensity of the lines. Hence the fluorite structure of UO_2 persists without significant change in cell dimension. The evidence favours the view that they are single-phase materials, and not mixtures of UO_2 with a higher oxide. (i) There is no *X*-ray evidence for the presence of a second phase throughout this composition range. Neither the change of intensity with composition nor the diffuseness of the diffraction patterns indicates that such oxides are made up of mixtures of unchanged UO_2 with amorphous oxidised material. (ii) The kinetics of the oxidation process follow the course of a reaction

Composition.	Detail of preparation.			Phases present.	Cell dimensions.	
	Temp.	Time of heating.	Nature of preparation.		*a*.	*c*.
$UO + UO_2$	1300°	15 min.	Continuously evacuated system	UO + α	5·457	—
$UO + UO_2$	1300	15 min.	,,	UO + α	5·455	—
$UO + UO_2$	1385	1 hr.	,,	UO + α	5·458	—
$UO_{2\cdot000}$	—	—	Starting material	α	5·456	—
$UO_{2\cdot036}$	131	—	End-product of kinetic run	α	5·457	—
$UO_{2\cdot044}$	170	—	,,	α	5·458	—
$UO_{2\cdot044}$	1000	1 hr.	Continuously evacuated system	β	5·428	—
$UO_{2\cdot075}$	1000	1000 hrs.	Evacuated sealed silica tube	α + β	5·458 5·433	—
$UO_{2\cdot092}$	180	—	End-product of kinetic run	α	5·456	—
$UO_{2\cdot092}$	750	3 hrs.	Continuously evacuated system	α + β	5·457 5·441	—
$UO_{2\cdot092}$	1000	1 hr.	,,	α + β	5·457 5·432	—
$UO_{2\cdot092}$	1520	½ hr.	,,	α	5·458	—
$UO_{2\cdot092}$	1235	1 hr.	,,	α	5·458	—
$UO_{2\cdot100}$	160	30 hrs.	End-product of kinetic run	α	5·457	—
$UO_{2\cdot116}$	200	—	,,	α	5·456	—
$UO_{2\cdot116}$	1000	1000 hrs.	Evacuated sealed silica tube	α + β	5·460 5·436	—
$UO_{2\cdot129}$	180	—	End-product of kinetic run	α	5·455	
$UO_{2\cdot133}$	168	—	,,	α	5·457	—
$UO_{2\cdot142}$	180	—	,,	α	5·452	—
$UO_{2\cdot180}$	165	—	,,	α	5·456	—
$UO_{2\cdot190}$	200	—	,,	α	5·456	—
$UO_{2\cdot190}$	1000	1000 hrs.	Evacuated sealed silica tube	β	5·433	—
$UO_{2\cdot190}$	2050	15 min.	Continuously evacuated system	α	5·457	—
$UO_{2\cdot210}$	175	8 hrs.	End-product of kinetic run	α + (γ)	5·457	—
$UO_{2\cdot210}$	750	3 hrs.	Continuously evacuated system	α	5·457	—
$UO_{2\cdot210}$	1000	1 hr.	,,	(α) + β	5·459 5·431	—
$UO_{2\cdot230}$	120	—	End-product of kinetic run	γ	—	—
$UO_{2\cdot23}$	120	—	,,	γ (19 cm.)	5·429	5·482
$UO_{2\cdot236}$	210	—	,,	α + U_3O_8	5·459	—
$UO_{2\cdot254}$	180	—	,,	γ	—	—
$UO_{2\cdot254}$	180	—	,,	γ (19 cm.)	5·420	5·525
$UO_{2\cdot260}$	170	140 hrs.	,,	γ	—	—
$UO_{2\cdot260}$	1000	1000 hrs.	Evacuated sealed silica tube	β + U_3O_8	5·428	—
$UO_{2\cdot260}$	1000	1 hr.	Continuously evacuated system	β + U_3O_8	5·428	—
$UO_{2\cdot290}$	120	—	Withdrawal from kinetic run	γ (19 cm.)	5·397	(5·550)
$UO_{2\cdot292}$	120	—	,,	γ	—	—
$UO_{2\cdot303}$	175	96 hrs.	End-product of kinetic run	γ	—	—
$UO_{2\cdot303}$	1000	1 hr.	Continuously evacuated system	β + U_3O_8	5·428	—
$UO_{2\cdot303}$	175	96 hrs.	End-product of kinetic run	γ (19 cm.)	5·386	5·554
$UO_{2\cdot304}$	210	—	,,	γ	—	—
$UO_{2\cdot304}$	500	64 hrs.	Evacuated sealed Pyrex tube	β + U_3O_8	5·426	—
$UO_{2\cdot304}$	1000	1000 hrs.	Evacuated sealed silica tube	β + U_3O_8	5·430	—
$UO_{2\cdot304}$	1000	1 hr.	Continuously evacuated system	β + U_3O_8	5·431	—

having diffusion within the solid phase as the rate-determining step, rather than the kinetics of a reaction proceeding at an interface between two phases (see below). (iii) The extent to which oxidation proceeds at low temperatures is strongly suggestive that nucleation of a second solid phase is not necessary. Our results agree entirely with those of Jolibois in that the oxidation process at temperatures up to 200—300° proceeds without discontinuity up to the composition $UO_{2\cdot3}$ and then ceases, although such an oxide is in no way in equilibrium with the oxygen of the atmosphere. Hence, the further oxidation of $UO_{2\cdot3}$ must involve some step associated with a measure of chemical inertia. This step may probably be identified as that of nucleation with a new structure, namely, that imposed by the different arrangement of uranium atoms in the U_3O_8 ($-U_2O_5$) phase. Reaction up to that point can proceed by way of a diffusion process within the solid phase; reaction beyond that point involves establishing nuclei of U_3O_8.

(II) *Low-temperature Oxides in the Range* $UO_{2\cdot20}$ *to* $UO_{2\cdot30}$.—The diffraction patterns of oxides having compositions between $UO_{2\cdot2}$ and $UO_{2\cdot3}$ can, as stated by Jolibois (*loc. cit.*), be described as that of UO_2 with extra lines. The changes in intensity, and the position of the additional lines indicate that (*hhh*) lines are intact, whereas (*hkl*) lines are split up into several components. The photographs can, in fact, be satisfactorily indexed in terms of a tetragonal structure with c/a ratio close to unity, and changing progressively with composition. The relation between cell dimensions and composition is summarised graphically in Fig. 1. A characteristic feature is the constant length of the cell diagonal, which is made up additively of $2(r_U + 2r_O)$. At the same time, the volume of the unit cell shows a small, but real, tendency to shrink from the value $162\cdot6 \pm 0\cdot5$ XU.^{3} for UO_2 to $161\cdot1 \pm 0\cdot5$ XU.^{3} for $UO_{2\cdot303}$.

The tetragonal structure was not observed for any oxide lower than $UO_{2\cdot20}$, the first evidences of the characteristic changes in contour and intensity of the diffraction lines being observed with an oxide of that composition. Extrapolation of the data in Fig. 1 suggests that c/a would be unity at about $UO_{2\cdot19}$. It is not clear whether, in the oxidation process, there is a continuous transition between the cubic and the tetragonal phases or whether there is a phase discontinuity at about $UO_{2\cdot2}$. It is quite possible that the tetragonal cell recorded is not the true cell, but no diffraction lines corresponding to a larger cell have been observed experimentally.

FIG. 1.

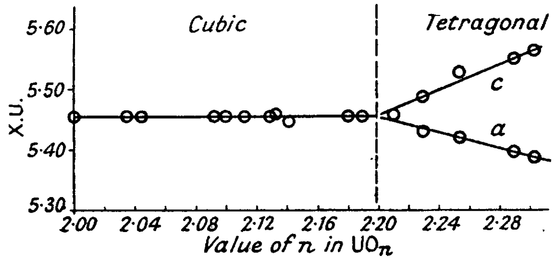

The oxidation of UO_2 at low temperatures thus forms, successively, two closely related non-stoicheiometric phases: the cubic oxides $UO_{2\cdot0}$–$UO_{2\cdot2}$ and the tetragonal oxides $UO_{2\cdot2}$–$UO_{2\cdot3}$. Both of these are to be considered as defect structures, containing a stoicheiometric excess of oxygen which might be incorporated in either of two ways: (*a*) by omission of a proportion of cations, or (*b*) by the incorporation of interstitial oxygen ions.

The third general mode of accommodating an excess of one component—substitutional solid solution, with oxide ions occupying lattice sites proper to uranium cations—can safely be ruled out of consideration in a polar structure of this kind. Defect structures based on the fluorite crystal lattice have already been extensively studied, in the form of anomalous mixed crystals between compounds of the types AB_2 and $AB_{1\cdot5}$ (anion deficiency) or AB_2 and AB_3 (anion excess, as compared with the ideal structure AB_2). There is, as pointed out by Zintl and Croatto (*Z. anorg. Chem.*, 1939, **242**, 79), a considerable weight of evidence for the view that in all these defect structures the cation lattice is substantially perfect, the variation of cation : anion ratio being produced either by incomplete occupation of anion lattice positions, or by incorporation of the excess of anions in interstitial positions.

Discrimination between these alternative modes of accommodating the stoicheiometric excess of oxygen is, in principle, unambiguously possible, by combining the observed density and cell dimensions of the material; this method was employed by Zintl and Croatto (*loc. cit.*) for the CeO_2–La_2O_3, and by Zintl and Udgård (*Z. anorg. Chem.*, 1939, **240**, 150) for the CaF_2–YF_3

and the CaF_2–ThF_4 mixed-crystal systems, which illustrate the two types of defective anion lattice referred to. Satisfactory density data for the low-temperature uranium oxides are, however, not available. Grønvold and Haraldsen (*loc. cit.*), from the apparent density of their tetragonal oxide (10·0), concluded that it represented a substitutional solid solution. We have, however, found the apparent density of authentic UO_2, measured with xylene as pyknometric liquid, to be 10·0 or 10·1, as compared with the *X*-ray density 10·96. Biltz and Müller (*loc. cit.*), on the other hand, obtained satisfactory densities for oxides ignited at 900—1300°, and it is probable that the low apparent density of UO_2 obtained by reduction at relatively low temperatures, and of the black oxides obtained by oxidation of such UO_2, is associated with the secondary structure of the oxide particles. The 5-μ. particles of our original UO_2 would necessarily contain capillary spaces of size comparable with that of the primary crystallites of UO_2—*i.e.*, 0·1—0·2 μ. and less—and it would appear that penetration and complete filling of the micro-capillaries by the pyknometric liquid cannot be achieved. Helium density measurements, which should overcome this difficulty, are not yet available.

We consider, accordingly, that by analogy with other anomalous fluorite mixed-crystal systems, the excess of oxygen enters the available interstitial positions ($\frac{1}{2}$00), etc., in which it may be accommodated in 6-fold co-ordination with uranium and with but little local distortion of the structure. If all ($\frac{1}{2}$00) sites could be occupied, the composition of the unit cell would be raised to U_4O_{11}—*i.e.*, $UO_{2\cdot75}$. In fact, the interstitial oxygen atoms are distributed at random, maintaining cubic symmetry, if less than 25% of the available sites are occupied, then tend to segregate into one set of ($\frac{1}{2}$00) positions, so conferring tetragonal symmetry, and finally " saturate " the structure when about 40% of interstitial sites are filled. It is noteworthy that throughout the existence range of the cubic phase there is no appreciable change in the dimensions of the unit cell, which actually shrinks progressively in the existence range of the tetragonal phase. The conclusion drawn by Rundle, Baenziger, Wilson, and MacDonald (*loc. cit.*) that shrinkage of the cell is incompatible with defect in the anion lattice, is however unwarranted, and ignores evidence already extant for fluorite structures. Incorporation of a stoicheiometric excess of oxygen implies simultaneous replacement of a corresponding proportion of U^{4+} cations by the smaller U^{6+} cations. The net effect on cell dimensions is determined by the interplay of the sizes and charge of the substituted cations with the distortion caused by interstitial anions. If the two sorts of cation are of the same or closely similar radius, the lattice distortion predominates and the cell expands as the anion : cation ratio is increased. This is, for example, the case with the SrF_2–YF_3 mixed crystals (Zintl and Udgård, *loc. cit.*; Ketelaar and Willems, *Rec. Trav. chim.*, 1937, **56**, 29), and the CaF_2–ThF_4 system (Zintl and Udgård, *loc. cit.*) and the cubic phase of the La_2O_3–LaOF system (Croatto, *Gazzetta*, 1943, **73**, 257). If, however, the substituted cation is appreciably smaller, as well as bearing a higher charge, these effects may outweigh the readjustment of positions imposed upon the anions when the ($\frac{1}{2}$00) positions are occupied. This is the case with the β-PbF_2–BiF_3 system (*idem, ibid.*, 1944, **74**, 20); the cell dimensions shrink from $a = 5{\cdot}927$ A. for β-PbF_2 to $a = 5{\cdot}901$ A. for mixed crystals with 33 mols.-% of BiF_3, and to $a = 5{\cdot}849$ A. for BiF_3 itself. In the system considered here, and for the occupation of not more than 25% of interstitial anion sites, the effects may approximately compensate.

(III) *High-temperature Oxides.*—Oxides in both the composition ranges described break up into two-phase systems when they are annealed at temperatures appreciably above the temperatures of their formation. The non-stoicheiometric phases are either completely metastable, or at least unstable above about 250°, with respect to three stable phases. (i) UO_2 proper; (ii) a clearly defined phase having a composition close to $UO_{2\cdot2}$ and referred to in the table on p. S 305 as the β-phase, and (iii) U_3O_8.

(i) *The* UO_2 *phase* (α-*phase*). Oxides intermediate between $UO_{2\cdot0}$ and $UO_{2\cdot19}$ split up into UO_2 and the β-phase. The presence of brown UO_2 as such is revealed by the distinctly ruddy tinge and the brown streak of such oxides after very prolonged annealing at high temperatures; the oxidation of UO_2 at low temperatures is attended by an immediate colour change to intense blue-black. The cell dimension of UO_2 in annealed oxides within this composition range is identical with that found for oxide preparations in which UO_2 co-exists with UO.* Whilst it appears that, for this particular system, arguments based upon cell dimensions may not be conclusive, it is probable that at high temperatures UO_2, is, in fact, a phase of practically constant composition.

---

* The preparations listed in the table on p. S 305, containing UO_2 + UO, were fired at only 1300°. It may well be that the UO_2 phase co-existing with UO at temperatures above 2000° is significantly deficient in oxygen, having an expanded cell as found by Rundle, Baenziger, Wilson, and MacDonald.

(ii) *The β-phase.* The β-phase is also a cubic phase, with a pseudo-fluorite structure and cell dimensions ($a = 5{\cdot}430 \pm 0{\cdot}003$ XU.) close to those of UO_2 ($a = 5{\cdot}457 \pm 0{\cdot}002$ XU.), so that it appears in the duplex specimens only in the close doubling of higher-angle diffraction lines. The oxide $UO_{2{\cdot}19}$ appeared to be single-phase after annealing. Oxides of lower compositions break up into mixtures of the α- and the β-phase, whilst the tetragonal oxides yield U_3O_8 + β-phase; hence the composition of the β-phase is close to $UO_{2{\cdot}19}$, and is probably definite. This composition would correspond to a true unit cell having a composition around U_6O_{13} or U_9O_{20}. This phase, may, therefore, be compared with the oxides of complex but well-defined composition recently identified in several other oxide systems, notably those of molydenum and vanadium. In the latter, Aebi (*Helv. Chim. Acta*, 1948, **31**, 8) has identified the oxide $V_{12}O_{26}$, and Magneli has determined the structure of the oxides Mo_8O_{23} and Mo_9O_{26}. In each case the composition of the true unit cell was ascertained from *X*-ray examination of single crystals. In the present instance, however, we have been unable to obtain crystals suitable for structure determination either by prolonged annealing or by sublimation (see below).

These analogous compounds, of which the crystal structures have been determined in detail, point to a possible structural relationship between the β-phase and the non-stoicheiometric phases formed at low temperatures. In the latter the excess of oxygen is incorporated interstitially; if the analogy with the other systems is correct, this disordered structure must change on annealing to an ordered structure in which uranium cations are situated in the co-ordination polyhedra of a close-packed or (to provide eight-fold co-ordination about the cations) a simple cubic lattice of oxygen atoms. The composition would then be determined by the periodic omission of cations from the structure, and the transformation which occurs on annealing could be represented by

$$UO_{2+x} \xrightarrow{\text{annealed at high temperatures}} U_{1-y}O_2$$

It must, however, be conceded that the densities recorded by Biltz and Müller for oxides $UO_{2{\cdot}15}$—$UO_{2{\cdot}21}$ are in better agreement with an " interstitial " than with a " subtractive " structure. The β-phase can be linked directly with the work of Biltz and Müller, who found a distinct discontinuity in the reduction or degradation of higher oxides at a composition near to $UO_{2{\cdot}2}$. They found, moreover, that oxides containing oxygen in excess of UO_2 were perceptibly volatile in a high vacuum and the sublimate had a composition approximating to $UO_{2{\cdot}14}$—$UO_{2{\cdot}17}$; the analytical data are probably not very precise. We have confirmed this observation, and have found that the black sublimate has, in fact, the cell dimensions of the β-phase. The material condensed on a cold silica tube showed no signs of the U_3O_8 structure, as might be expected if the volatile species were actually UO_3 which then underwent dissociation when it condensed. This suggests that the β-phase sublimes as such, and although this conclusion is surprising, it may perhaps be coupled with the apparent existence of $V_{12}O_{26}$ units in solution in fused V_2O_5, as cited by Aebi.

(iii) *The oxidation process.* The features of the oxidation of UO_2 can now be interpreted in terms of the foregoing observations. At low temperatures, oxygen may be incorporated interstitially up to the limits of composition of the tetragonal phase and the process then comes to a stand-still. In oxides at temperatures above about 250°, or if the temperature rises above this limit through the heat of reaction, the tetragonal phase breaks up into the β-phase + U_3O_8 (or possibly at these temperatures into the α-phase + U_3O_8). The system is thereby nucleated with the U_3O_8 phase, and oxidation can proceed to completion. The temperature of renewed oxidation, as was found by Jolibois, is probably the temperature at which the tetragonal phase breaks down, for in none of our experiments was the tetragonal phase observed in oxides prepared at temperatures appreciably in excess of 220°.

Kinetics of the oxidation of uranium dioxide.

The oxidation of uranium dioxide is remarkable for the speed with which it takes place at relatively low temperature. The results given here summarise a preliminary study of this process; a fuller investigation of several features revealed by this work will be published later.

The dioxide, spread in a thin layer over a shallow silica or aluminium dish, was oxidised in air, in a thermostated oven at temperatures between 120° and 175°, and in a steam-jacketed tube for prolonged periods at 100°. The increase in weight after successive time intervals was measured directly. Oxidation then took place at constant oxygen pressure; at higher temperatures the rate of the initial oxidation process was so great that gaseous diffusion became the rate-controlling step. The method adopted in these preliminary experiments made it impossible to follow the earliest stages of the reaction except at the lowest temperatures; it was, however, convenient for studying the process between about 15% and 90% of total conversion.

The reaction was characterised by an extremely rapid initial stage, declining regularly according to a roughly parabolic law, suggestive of a typical diffusion-controlled process (Fig. 2).

FIG. 2.

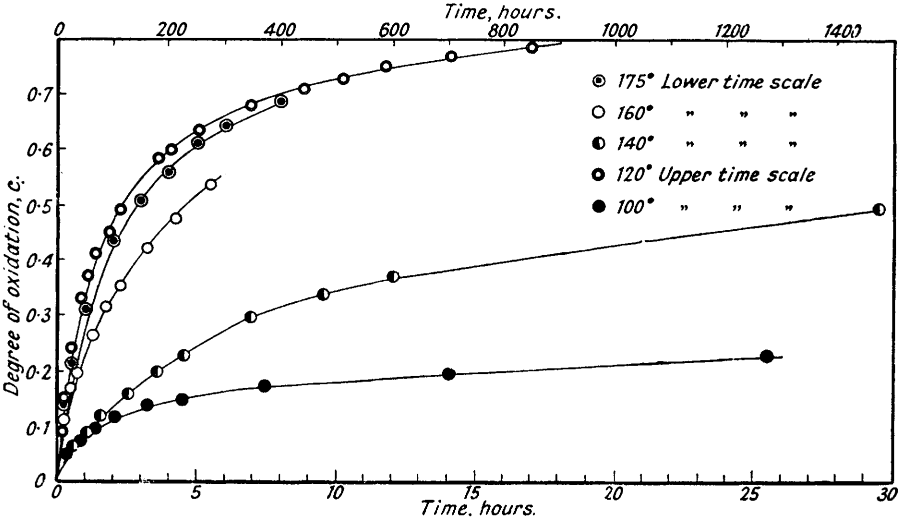

Discussion.—Reactions of the general type $A_{solid} + B_{gas} \longrightarrow C_{solid}$ may conveniently be divided into two types, according as the rate-controlling step is (*a*) the phase-boundary reaction, or (*b*) the transport of reactant to the phase boundary by diffusion in either the solid or the gaseous phase.

Type (*a*). Phase-boundary controlled reactions, involving the movement of the A–C interface through each particle, have frequently been encountered in the reactions of solids. The rate of such a process will then be proportional to the area of the interface at each instant. The system may be idealised by assuming the solid to consist of spherical particles of uniform size, with reaction starting at $t = 0$ on all particles; that the reaction considered here shows no phase of initial acceleration indicates that, in fact, nucleation is not a rate-determining step. Then if at time t the fraction c of each particle has undergone reaction, we have

$$dc/dt = k(1 - c)^{2/3} \quad . \quad . \quad . \quad . \quad . \quad . \quad . \quad . \quad . \quad . \quad (1)$$

i.e.,

$$(1 - c)^{1/3} = 1 - k^1 t \quad . \quad . \quad . \quad . \quad . \quad . \quad . \quad . \quad . \quad . \quad (2)$$

It is convenient to plot, as in Fig. 3, the degree of conversion c as a function of $r = t/t_{1/2}$, a reduced time scale permitting comparison with observations made at any temperature. From Fig. 3, curve *A*, it is apparent that the law of the phase-boundary reaction does not reproduce the observed kinetic features of the oxidation process.

Type (*b*). For diffusion-controlled reactions, two classes of system may be formally recognised. (i) If the solid compound *A* has a wide range of composition, so that the reaction does not give rise to the formation of a new phase, a composition gradient will be established through each grain as reaction proceeds. This may well be the case for the oxidation of UO_2. The composition of the oxide along any radius of the idealised particle is initially uniform, $UO_{2\cdot00}$; after a time t, the composition will vary along the radius from the fully oxidised state at the surface to unaltered material at the centre. The distribution of composition is formerly similar to the distribution of temperature in a spherical particle immersed in a heated environment; the kinetics of the reaction are determined by the diffusion of reactant through the particle, and the appropriate solution of the diffusion equation can be taken from the analogous case of the conduction of heat. Denoting the composition at time t as X_t, the initial composition as X_i, and the ultimate composition as X_f, we have

$$\frac{X_t - X_i}{X_f - X_i} = 1 - \frac{6}{\pi^2} \sum_1^\infty \frac{1}{n^2} e^{-n^2 Dt/a^2} = c, \text{ the fraction of conversion} \quad . \quad . \quad . \quad (3)$$

where a is the radius of the spherical particle and $n = 1, 2, 3 \ldots . \infty$. The variation of conversion c with time is shown, with the reduced time scale $r = t/t_{1/2}$, by curve *B*, Fig. 3.

(ii) Whilst the supply of reactant by a diffusion process may be the rate-controlling factor, if the product of reaction B constitutes a new phase, the reaction takes place at the A–C interface, which changes progressively in area as it moves through the particle. The kinetic laws of processes of this kind have been discussed by Valenci (*Compt. rend.*, 1936, **202**, 309) and Peschanski (*Ann. Chim.*, 1947, **2**, 599). If d_0, M_0, and d_i, M_i are the density and formula weight of the initial material and of the product, respectively, and H is the concentration difference between the interfaces leading to diffusion, they find

$$\frac{2\,DHM_0}{d_0a^3}t = \frac{r}{r-1} - (1-c)^{2/3} - \frac{1}{r-1}[1+(r-1)c]^{2/3} \quad . \quad . \quad . \quad . \quad . \quad (4)$$

where a = initial radius of each particle, D = diffusion coefficient, and c = degree of conversion, as before, and $r = M_id_0/M_0d_i$. This expression would be valid if, in fact, the oxidation of UO_2 proceeded by way of a non-stoicheiometric phase (*e.g.*, the tetragonal phase), differing from UO_2, but not detected by X-ray methods in the oxides $UO_{2\cdot0}$—$UO_{2\cdot2}$ by reason of its poor crystallinity or other reasons.

FIG. 3.

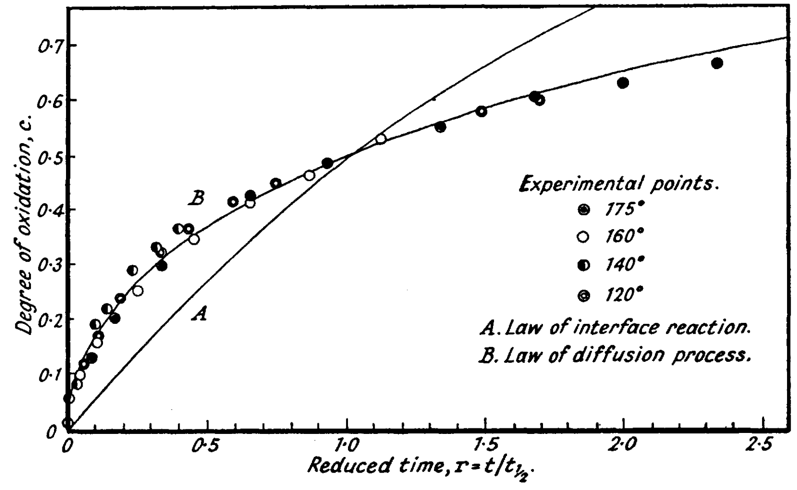

Evaluation of the right-hand side of equation (4), using the experimental data, gives fairly good linear reactions between $f(c)$ and time for a considerable proportion of the total reaction; it would appear, however, that the expression is not very sensitive to changes in r (which in the present instance is uncertain) or other parameters involved in evaluating the experimental data.

In general, it may be concluded that the oxidation process is fairly well represented as a reaction of type (*b*) (i), involving a composition gradient through particles of a non-stoicheiometric oxide. The fit is not so satisfactory for the initial stages of the reaction, and at least two reasons may be advanced for deviations from the idealised law of equation (3). The assumption of uniform spherical particles is obviously not justified; the effective size of the particles will be distributed about some mean. The effective radius, as a diffusion path, enters into equation (3) in such a way, however, that the time scale for small particles is telescoped, as compared with that for the larger, and in any assembly of particles of different size the apparent diffusion constant (calculated for a mean radius a) must fall off with time, as the net reaction proceeds. A second factor causing deviation from the simple diffusion law arises from the small particle size. With cubic crystals of UO_2 of about 0·1 μ. size, it may be seen that approximately 3% of all the unit cells in each crystallite lie exposed on the exterior faces; the rate of the earliest stages in the oxidation will accordingly be determined only by the rate of a chemisorption process, without involving diffusion within the solid. There is, indeed, evidence that under certain conditions the diffusion process is not the unique rate-determining step. At higher temperatures the lower activation energy for the chemisorption step, as compared with that for diffusion, may make the phase-boundary process no longer rapid compared with diffusion. It has, in fact, been observed that the rate of the reaction is not independent of the oxygen pressure at 160—180°, when the oxygen pressure is reduced below 100 mm. A fuller discussion of these points is reserved for a later publication.

The results of the preliminary series of gravimetric measurements of reaction rate are summarised in Fig. 2 and the table below; this lists the mean diffusion coefficient as calculated from the time for 50% conversion of $UO_{2\cdot0}$ into $UO_{2\cdot30}$. These data indicate an activation energy of 27 kcals. for the reaction, a value which appears of reasonable magnitude for a diffusion process within the solid phase.

Temp.	175°	160°	140°	120°	100°
D	$4\cdot1 \times 10^{-16}$	$2\cdot4 \times 10^{-16}$	$4\cdot05 \times 10^{-17}$	$1\cdot05 \times 10^{-17}$	10^{-19}

We are indebted to several colleagues, and in particular to Mr. R. C. Blakey, for assistance in several sections of the experimental work. This work is published by permission of the Director of the Atomic Energy Research Establishment, Ministry of Supply.

ATOMIC ENERGY RESEARCH ESTABLISHMENT,
HARWELL, DIDCOT, BERKS.

[*Read, March* 30*th*, 1949.]